Advances in Bioresearch
Adv. Biores., Vol 17 (2) February 2026: 227-238

Print ISSN 0976-4585; Online ISSN 2277-1573
Journal's URL:http://www.soeagra.com/abr.html
CODEN: ABRDC3
DOI: 10.15515/abr.0976-4585.17.2.227238

Advances in Bioresearch

ORIGINAL ARTICLE

Molecular Docking, ADME Studies of 2-(4-Phenyl-1*H*-1,2,3-Triazol-1-YL)-1,8-Naphthyridines

Golla Mandala Soujanya [1], **Thipirisetty Shiva Chander** [1], **Sreelatha Beemagani**[2*]
[1] Research Scholar, Chaitanya (Deemed to be University), Himayat Nagar, Hyderabad 500075, Telangana, India
[*2] Department of Microbiology, Chaitanya (Deemed to be University), Himayat Nagar, Hyderabad 500075, Telangana, India
***Corresponding author email:** bslathabathini@gmail.com

ABSTRACT
The development of novel antibacterial agents targeting essential bacterial enzymes is an important strategy to overcome antimicrobial resistance. In the present study, a series of 2-(4-phenyl-1H-1,2,3-triazol-1-yl)-1,8-naphthyridine derivatives (4a–4i) were evaluated using molecular docking and in silico ADME analysis to explore their potential as inhibitors of Escherichia coli DNA gyrase B. Molecular docking studies were carried out against DNA gyrase B (PDB ID: 6KZV) to investigate the binding affinity and interaction profile of the synthesized compounds. All derivatives exhibited favorable binding energies ranging from –8.32 to –9.79 kcal/mol, indicating strong interaction with the active site of the enzyme. Among the studied compounds, compound 4g showed the highest binding affinity (–9.79 kcal/mol) with the lowest inhibition constant (67.04 nM), suggesting strong inhibitory potential. Compound 4i also demonstrated significant binding with a docking score of –8.81 kcal/mol. Interaction analysis revealed that compound 4h formed two hydrogen bonds with THR165 and VAL167, whereas compounds 4a and 4d formed single hydrogen bonds with THR165 and ARG136, respectively. The ADME prediction indicated excellent intestinal absorption (98–100%) and moderate to high Caco-2 permeability (log Papp 1.05–2.03) for all compounds, suggesting good oral bioavailability. Several derivatives acted as CYP3A4 inhibitors, while CYP1A2 inhibition was predicted for all compounds and CYP2C9 inhibition for 4a, 4g, and 4i. Overall, compounds 4b, 4e, and 4f showed balanced ADME properties, whereas compound 4g emerged as the most promising DNA gyrase B inhibitor.
KEYWORDS: *1,8-Naphthyridines, ADME, Molecular Docking, Triazoles, E. coli, DNA gyrase B.*

Received 11.01.2026 Revised 30.01.2026 Accepted 23.02.2026

How to cite this article:
Golla Mandala S, Thipirisetty S C, Sreelatha B · Molecular Docking, ADME Studies of 2-(4-Phenyl-1*H*-1,2,3-Triazol-1-YL)-1,8-Naphthyridines. Adv. Biores. Vol 17 [2] February 2026. 227-238

INTRODUCTION

1,8-Naphthyridine is an important heterocyclic scaffold widely investigated in medicinal chemistry because of its diverse pharmacological properties. Structurally, the 1,8-naphthyridine nucleus consists of a bicyclic aromatic system containing two nitrogen atoms positioned at the 1 and 8 locations of the ring, which contributes to its strong binding interactions with various biological targets. According to previous reports, naphthyridine derivatives exhibit a broad spectrum of pharmacological activities, including anti-infective, anticancer, neurological, cardiovascular, and immunological effects (1,2). Due to these diverse biological properties, the naphthyridine framework has been extensively explored as a privileged scaffold in the design and development of new therapeutic agents.

Among the various derivatives, 4-oxo-1,8-naphthyridine-3-carboxylic acid represents the fundamental structural motif present in several commercially available antibacterial drugs. The earliest compound belonging to this class was reported by who discovered nalidixic acid, one of the first antibacterial agents containing the naphthyridine nucleus (3). Nalidixic acid exhibits potent antibacterial activity by selectively and reversibly inhibiting bacterial DNA replication. Its mechanism of action involves inhibition of the A subunit of bacterial DNA gyrase, an enzyme essential for controlling DNA supercoiling during bacterial replication and transcription (4). The discovery of nalidixic acid initiated extensive research into

naphthyridine-based antibacterial drugs and led to the development of several clinically important analogues.

Structural modification of the naphthyridine scaffold has resulted in compounds possessing improved pharmacological profiles and expanded therapeutic applications. For example, amfonelic acid, which is a 7-benzyl derivative of nalidixic acid, was initially identified for its antibacterial properties. However, subsequent studies revealed that it functions primarily as a potent dopaminergic stimulant, demonstrating the versatility of the naphthyridine core in interacting with different biological systems (5). This example illustrates that small structural modifications within the naphthyridine nucleus can significantly alter the biological activity and therapeutic applications of these compounds.

Another important derivative is enoxacin, chemically described as 1-ethyl-6-fluoro-4-oxo-7-(piperazin-1-yl)-1,4-dihydro-1,8-naphthyridine-3-carboxylic acid. The presence of a piperazine ring in its structure enhances both antibacterial potency and pharmacokinetic properties. Enoxacin exerts its antibacterial activity by inhibiting bacterial DNA gyrase and topoisomerase IV, thereby blocking bacterial DNA replication (6). In addition to its antimicrobial activity, enoxacin has also been reported to inhibit microRNA expression in various Gram-positive and Gram-negative bacteria. Structurally, enoxacin is an analogue of norfloxacin and is widely used for the treatment of infections such as gastroenteritis, respiratory tract infections, and urinary tract infections (7,8)

Naphthyridine-based antibiotics are also effective against a wide range of clinically relevant bacterial infections. These compounds have been used in the treatment of acute bacterial exacerbations of chronic bronchitis and mild to moderate community-acquired pneumonia. Pathogens commonly targeted by these agents include *Staphylococcus aureus, Streptococcus pyogenes, Haemophilus influenzae, Klebsiella pneumoniae, Legionella pneumophila, Moraxella catarrhalis, Chlamydia pneumoniae*, and *Mycoplasma pneumoniae* (9–13). Furthermore, several derivatives have demonstrated activity against multidrug-resistant strains of Streptococcus pneumoniae, highlighting their importance in addressing the growing problem of antimicrobial resistance.

Recent research efforts have also focused on the development of novel naphthyridine-based investigational antibiotics to combat multidrug-resistant infections. One such compound, 1-cyclopropyl-6-fluoro-1,4-dihydro-7-[8-(methoxyimino)-2,6-diazaspiro]-1,8-naphthyridine-3-carboxylic acid, has been reported as a promising antibacterial agent for the treatment of infections caused by Gram-positive bacteria and Neisseria gonorrhoeae (14–17).

In recent years, the incorporation of 1,2,3-triazole moieties into bioactive molecules has emerged as an effective strategy in medicinal chemistry because of their remarkable stability, ability to participate in hydrogen bonding, and favorable pharmacokinetic characteristics. The hybridization of biologically active scaffolds such as naphthyridine and 1,2,3-triazole may lead to compounds with enhanced biological activity and improved binding affinity toward biological targets. Therefore, molecular docking and ADME studies of 2-(4-phenyl-1H-1,2,3-triazol-1-yl)-1,8-naphthyridine derivatives are valuable for predicting their binding interactions with target proteins and evaluating their drug-likeness and pharmacokinetic properties, thereby facilitating the identification of promising therapeutic candidates.

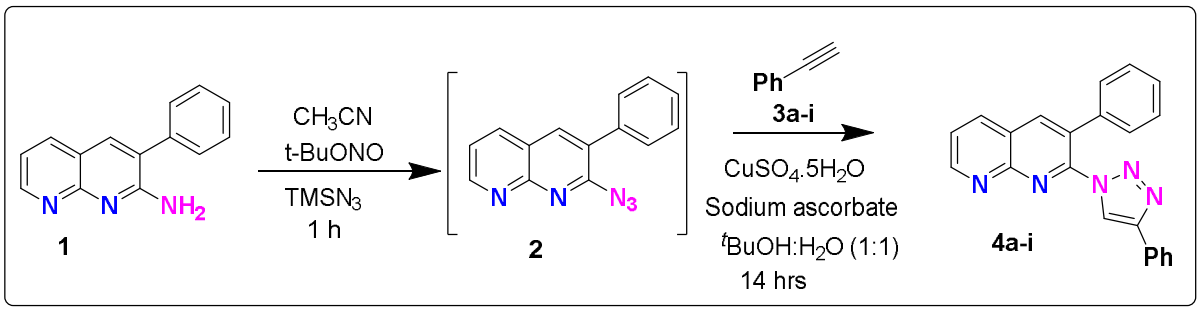

Scheme 1: Synthesis of 2-(4-phenyl-1H-1,2,3-triazol-1-yl)-1,8-naphthyridines 4a-i

MATERIAL AND METHODS

Molecular Docking studies

Molecular docking studies were performed to evaluate the binding affinity and interaction profile of the synthesized 2-(4-phenyl-1H-1,2,3-triazol-1-yl)-1,8-naphthyridine derivatives (4a–4i) with the target enzyme DNA gyrase B of Escherichia coli. The three-dimensional crystal structure of DNA gyrase B was obtained from the Protein Data Bank (PDB ID: 6KZV). Prior to docking (18). the protein structure was prepared by removing water molecules and other co-crystallized ligands, followed by the addition of

hydrogen atoms and appropriate charge assignments (19,20). The chemical structures of the synthesized compounds were constructed and optimized before docking analysis. Docking simulations were carried out to predict the binding orientation and interaction pattern of each ligand within the active site of the target protein. The docking process evaluated binding energy, inhibition constants, hydrogen bonding interactions, and other non-covalent interactions such as hydrophobic contacts and van der Waals forces. The best docking conformations were selected based on the lowest binding energy values and favorable interaction with key active site residues. The interaction profiles and binding orientations of the docked complexes were further analyzed using 2D and 3D visualization tools to identify the amino acid residues involved in ligand binding. 2-(4-Phenyl-1H-1,2,3-Triazol-1-yl)-1,8-Naphthyridines are shown in Figure 1.

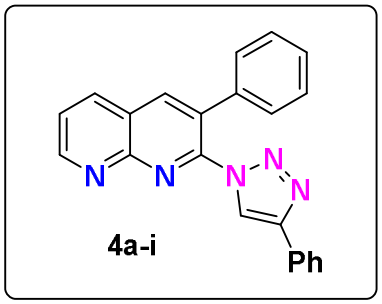

Figure 1: 2-(4-Phenyl-1H-1,2,3-Triazol-1-yl)-1,8-Naphthyridines

***In Silico* ADME Analysis**

The absorption, distribution, metabolism, excretion, and toxicity (ADMET) properties of the synthesized compounds 4a–4i were predicted using the pkCSM and SwissADME online platforms. These computational tools were employed to evaluate pharmacokinetic parameters and drug-likeness properties of the compounds. The predicted parameters included intestinal absorption, Caco-2 permeability, water solubility, volume of distribution (VDss), fraction unbound (Fu), blood–brain barrier permeability (BBB), and central nervous system (CNS) permeability.

Metabolic properties were assessed by predicting interactions with major cytochrome P450 enzymes including CYP3A4, CYP1A2, and CYP2C9, which play an important role in drug metabolism. Excretion parameters such as total clearance were also estimated. In addition, toxicity predictions including AMES mutagenicity, hERG inhibition, hepatotoxicity, skin permeability, and maximum tolerated dose were evaluated to assess potential safety concerns. Drug-likeness properties of the compounds were further analyzed using Lipinski, Ghose, Veber, Egan, and Muegge rules, along with lipophilicity estimation (Log P). These parameters provide an indication of oral bioavailability and pharmacokinetic suitability of the synthesized derivatives. The predicted ADME parameters were used to assess the overall pharmacokinetic behavior and drug-likeness profile of the studied compounds (21)(22).

RESULTS AND DISCUSSIONS

Molecular docking studies

Molecular docking studies of the synthesized compounds 4a–4i were carried out against DNA gyrase B of Escherichia coli (PDB ID: 6KZV) in order to evaluate their binding affinity and possible interactions within the active site of the enzyme. The structures and names of the selected compounds are presented in Table 1, while the docking results are summarized in Table 2. The docking results indicated that all compounds exhibited favorable binding affinities toward the target protein, with binding energies ranging from –8.32 to –9.79 kcal/mol, suggesting that the synthesized 2-(4-phenyl-1H-1,2,3-triazol-1-yl)-1,8-naphthyridine derivatives possess good interaction potential with the active site of DNA gyrase B.

Among the studied compounds, compound 4g demonstrated the highest binding affinity of –9.79 kcal/mol, accompanied by the lowest inhibition constant of 67.04 nM, indicating strong interaction with the enzyme. Compound 4i also showed a relatively high docking score of –8.81 kcal/mol, suggesting good binding capability compared with other derivatives in the series. These findings highlight the potential of these compounds as inhibitors of DNA gyrase B.

Analysis of the docking interactions revealed that several compounds formed hydrogen bonds with key amino acid residues present in the active site of the enzyme. Compound 4h formed two hydrogen bonds with THR165 and VAL167, indicating stable interactions within the binding pocket. In addition, compound 4a formed one hydrogen bond with THR165, whereas compound 4d established one hydrogen bond with ARG136. The observed hydrogen bond lengths ranged from 2.17 to 2.57 Å, suggesting stable and favorable interactions between the ligands and the protein residues. Interestingly, some derivatives such as 4b, 4c, 4e, 4f, 4g, and 4i exhibited significant binding affinities even in the absence of hydrogen

bond formation. This observation indicates that hydrophobic interactions and van der Waals forces may play an important role in stabilizing the ligand–protein complexes within the active site of DNA gyrase B. The key amino acid residues involved in ligand interactions were identified as THR165, VAL167, and ARG136, which play a crucial role in stabilizing the docked complexes. Overall, the docking results suggest that the synthesized derivatives exhibit promising inhibitory potential against DNA gyrase B, with compound 4g emerging as the most promising inhibitor among the studied series (Tables 1–3).

Table 1: Names & Structures of Selected Compounds 4a-4i

Entry	Name	Structure
4a	3-phenyl-2-(4-phenyl-1*H*-1,2,3-triazol-1-yl)-1,8-naphthyridine	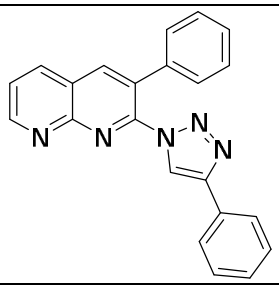
4b	3-phenyl-2-(4-(p-tolyl)-1*H*-1,2,3-triazol-1-yl)-1,8-naphthyridine	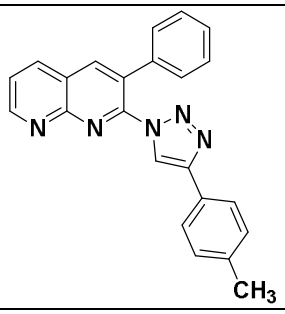
4c	2-(4-(4-methoxyphenyl)-1*H*-1,2,3-triazol-1-yl)-3-phenyl-1,8-naphthyridine	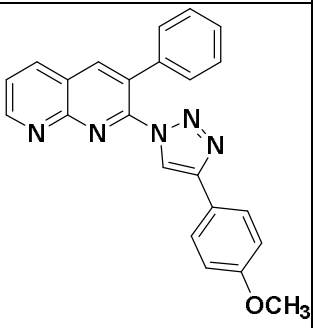
4d	2-(4-(4-nitrophenyl)-1*H*-1,2,3-triazol-1-yl)-3-phenyl-1,8-naphthyridine	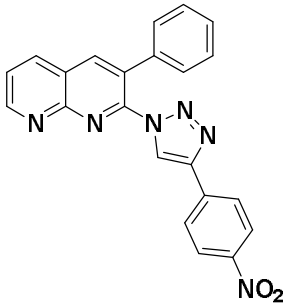

4e	2-(4-(4-chlorophenyl)-1*H*-1,2,3-triazol-1-yl)-3-phenyl-1,8-naphthyridine	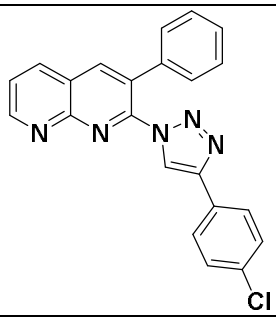
4f	2-(4-(4-bromophenyl)-1*H*-1,2,3-triazol-1-yl)-3-phenyl-1,8-naphthyridine	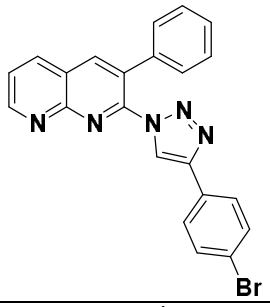
4g	2-(4-(4-cyclohexylphenyl)-1*H*-1,2,3-triazol-1-yl)-3-phenyl-1,8-naphthyridine	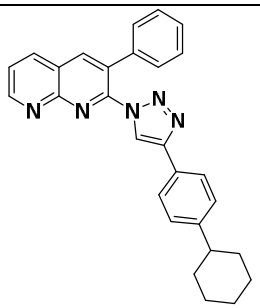
4h	4-(1-(3-phenyl-1,8-naphthyridin-2-yl)-1*H*-1,2,3-triazol-4-yl) benzonitrile	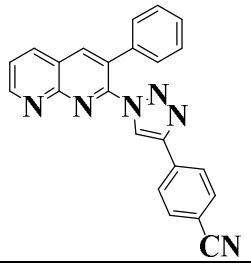
4i	2-(4-cyclohexyl-1*H*-1,2,3-triazol-1-yl)-3-phenyl-1,8-naphthyridine	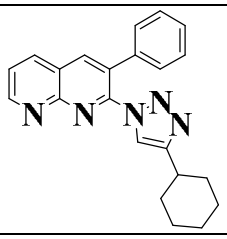

Table 2: Molecular docking results of compounds 4a-4i with *E. coli* DNA gyrase B (PDB ID-6KZV)

Entry	Binding Energy (kcal/mol)	Inhibition Constant	No. of Hydrogen Bonds	Residues Involved in Hydrogen Bonding (Bond length in Å)
4a	-8.66	451.40	1	THR165 (2.56)
4b	-8.50	587.27	–	–
4c	-8.32	796.23	–	–
4d	-8.61	486.77	1	ARG136 (2.17)
4e	-8.40	691.78	–	–
4f	-8.43	667.08	–	–
4g	-9.79	67.04	–	–
4h	-8.46	633.90	2	THR165 (2.57), VAL167 (2.44)
4i	-8.81	346.78	–	–

Table 3: 2D and 3D Binding interaction with *E. coli* DNA gyrase B

3D Interaction	2D Interaction
4a	
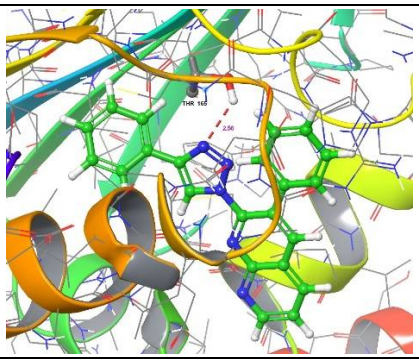	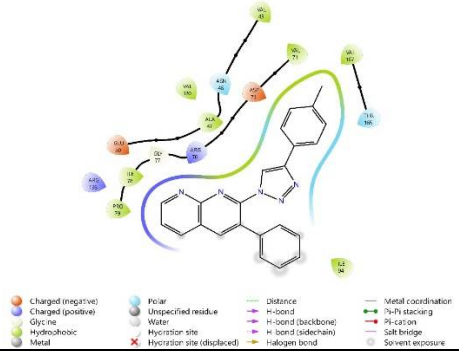
4b	
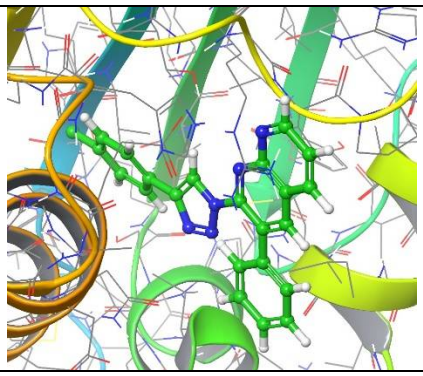	**Not Generate**
4c	
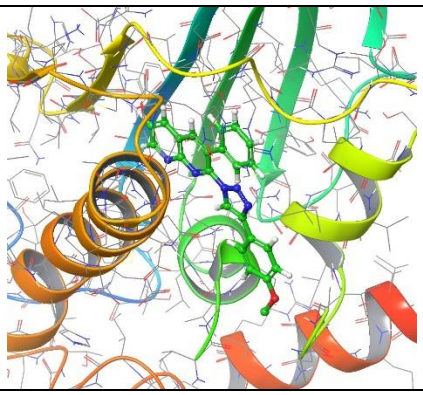	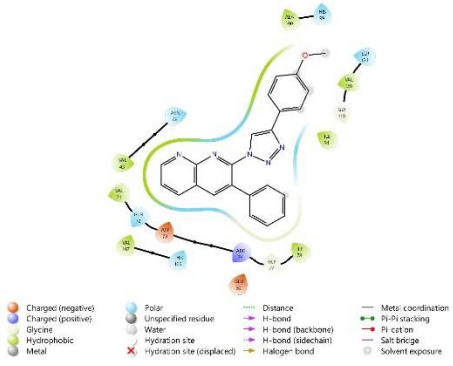
4d	

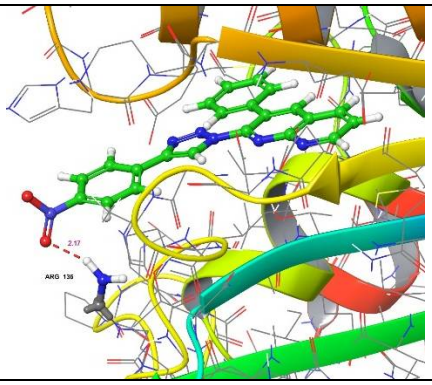
2.17
ARG 138

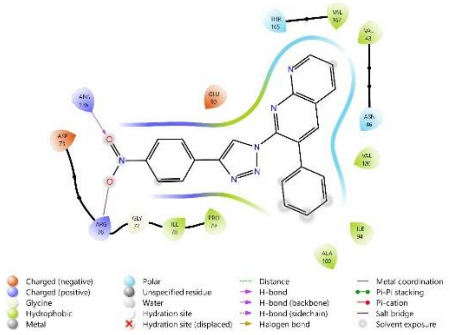
Charged (negative)
Charged (positive)
Glycine
Hydrophobic
Metal
Polar
Unspecified residue
Water
Hydration site
Hydration site (displaced)
Distance
H-bond
H-bond (backbone)
H-bond (sidechain)
Halogen bond
Metal coordination
Pi-Pi stacking
Pi-cation
Salt bridge
Solvent exposure

4e

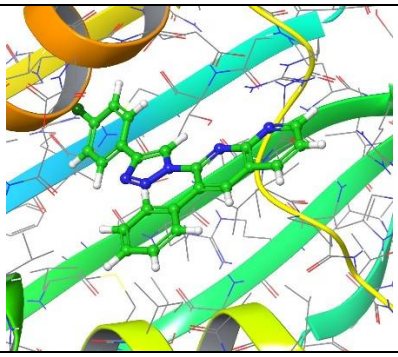

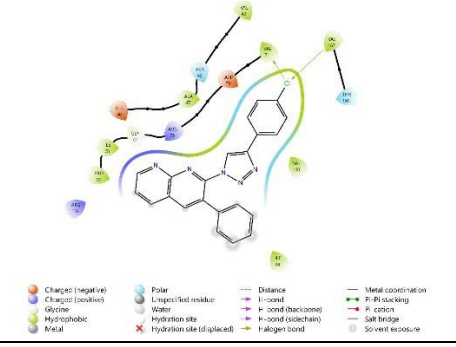
Charged (negative)
Charged (positive)
Glycine
Hydrophobic
Metal
Polar
Unspecified residue
Water
Hydration site
Hydration site (displaced)
Distance
H-bond
H-bond (backbone)
H-bond (sidechain)
Halogen bond
Metal coordination
Pi-Pi stacking
Pi-cation
Salt bridge
Solvent exposure

4f

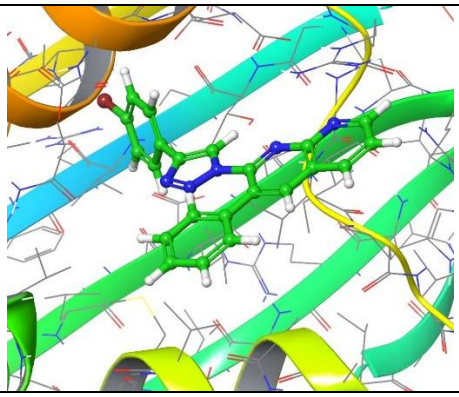

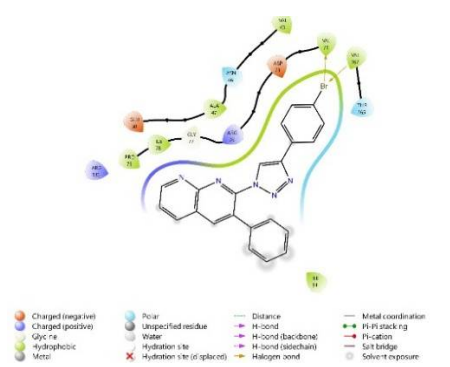
Charged (negative)
Charged (positive)
Glycine
Hydrophobic
Metal
Polar
Unspecified residue
Water
Hydration site
Hydration site (displaced)
Distance
H-bond
H-bond (backbone)
H-bond (sidechain)
Halogen bond
Metal coordination
Pi-Pi stacking
Pi-cation
Salt bridge
Solvent exposure

4g

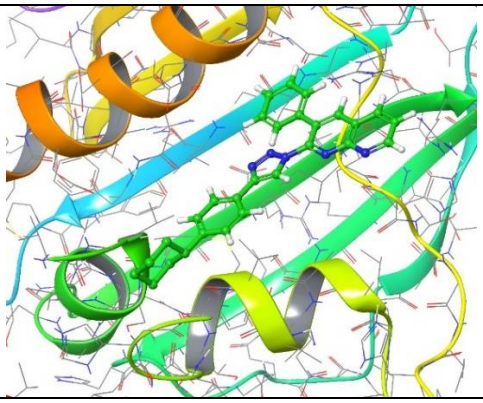

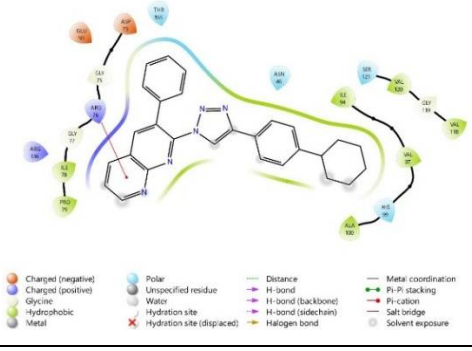
Charged (negative)
Charged (positive)
Glycine
Hydrophobic
Metal
Polar
Unspecified residue
Water
Hydration site
Hydration site (displaced)
Distance
H-bond
H-bond (backbone)
H-bond (sidechain)
Halogen bond
Metal coordination
Pi-Pi stacking
Pi-cation
Salt bridge
Solvent exposure

4h

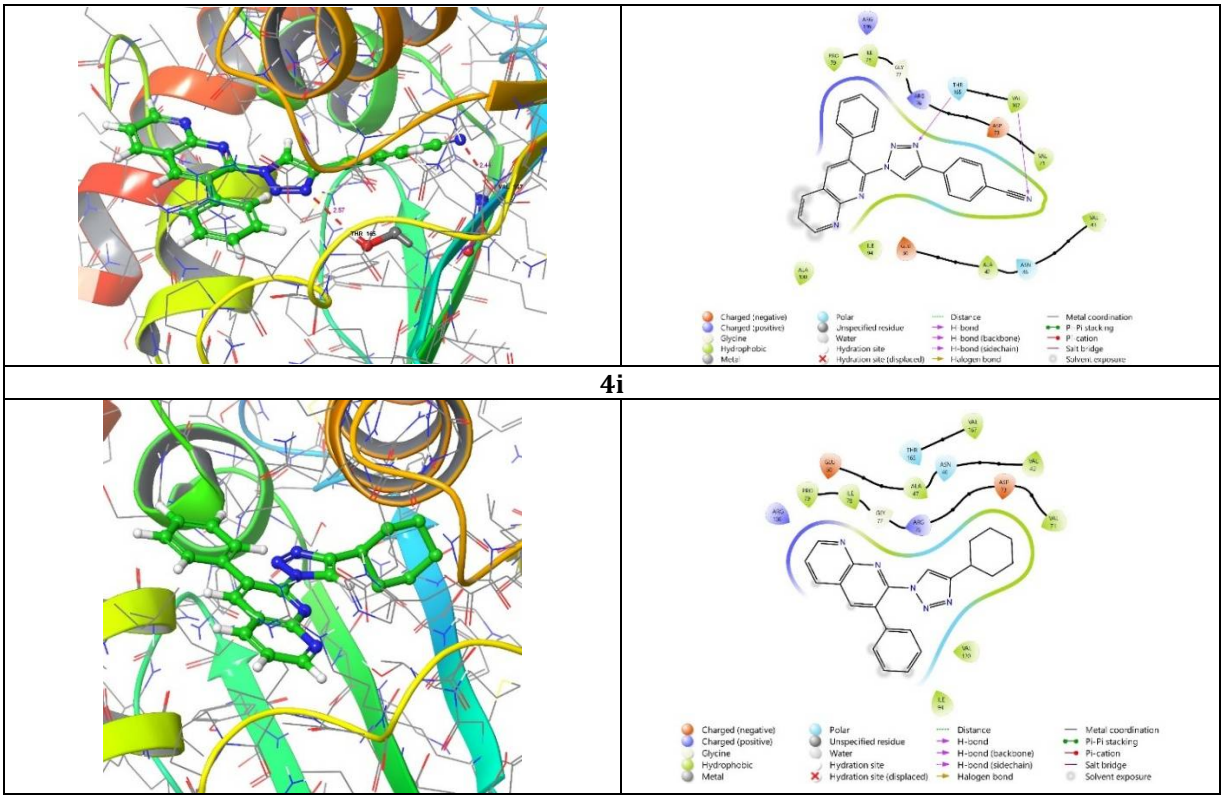

4i

***In Silico* pharmacokinetic profile (ADME)**

The in silico pharmacokinetic (ADME) properties of the synthesized compounds 4a–4i were evaluated using the pkCSM and SwissADME platforms in order to assess their drug-likeness and pharmacokinetic behavior. The predicted parameters included absorption, distribution, metabolism, excretion, toxicity, and drug-likeness characteristics. Overall, the computational results indicate that the synthesized 2-(4-phenyl-1H-1,2,3-triazol-1-yl)-1,8-naphthyridine derivatives possess favourable pharmacokinetic profiles with acceptable drug-likeness properties.

All compounds demonstrated excellent intestinal absorption ranging from 98–100%, suggesting good oral bioavailability potential. The predicted Caco-2 permeability values (log Papp 1.05–2.03) indicate moderate to high intestinal permeability for the series, with compound 4d showing the highest permeability (2.031). Water solubility predictions (Log S) suggested moderate solubility for most compounds; however, compounds 4g (−5.334) and 4a (−4.51) exhibited comparatively lower aqueous solubility.

The predicted volume of distribution (VDss) values ranged from 0.033 to 0.579 log L/kg, indicating moderate tissue distribution. Among the derivatives, compound 4i displayed the highest distribution profile, suggesting greater tissue penetration. The fraction unbound (Fu) values ranging from 0.237 to 0.317 indicate moderate plasma protein binding for the studied compounds. Analysis of blood–brain barrier permeability (log BB) revealed that compounds 4b, 4e, and 4f possess relatively higher brain penetration potential, whereas 4d and 4h showed limited BBB permeability. Furthermore, the predicted CNS permeability (log PS −1.339 to −2.253) values indicate generally low penetration into the central nervous system, which may help minimize potential CNS-related adverse effects.

Metabolism prediction indicated that most compounds act as substrates of the CYP3A4 enzyme, suggesting metabolism through this major hepatic cytochrome P450 pathway. In addition, several derivatives (4a, 4b, 4f, 4h, and 4i) were predicted to act as CYP3A4 inhibitors, which may potentially lead to drug–drug interaction concerns. CYP1A2 inhibition was predicted for all compounds, while CYP2C9 inhibition was observed for 4a, 4g, and 4i. The predicted excretion values (0.132–1.051 log ml/min/kg) suggest moderate clearance rates for the compounds, with 4b and 4h showing comparatively higher clearance profiles.

Toxicity prediction revealed that compound 4a showed AMES mutagenicity, whereas the remaining derivatives (4b–4i) were predicted to be non-mutagenic, indicating improved genetic safety for most compounds. None of the compounds were predicted to inhibit hERG I, suggesting a reduced risk of severe cardiotoxicity; however, all compounds except 4i showed hERG II inhibition, indicating a moderate

cardiotoxicity risk. All derivatives were predicted to exhibit hepatotoxicity, while none showed significant skin permeation liability. The predicted maximum tolerated dose values indicated that compounds 4e and 4f possess comparatively higher tolerance levels among the studied series.

Drug-likeness evaluation revealed that all compounds satisfied Lipinski's rule of five and Veber's rule, suggesting good oral drug-likeness and bioavailability potential. Most compounds also complied with the Ghose and Egan rules, whereas compound 4g violated both criteria. In addition, Muegge rule violations were observed for compounds 4e, 4f, 4g, and 4i, indicating minor limitations in drug-likeness properties. The predicted lipophilicity values (Log P 3.44–5.72) suggest moderate to high hydrophobicity, with compound 4g showing the highest lipophilicity among the series.

Overall, the ADMET analysis suggests that several derivatives, particularly compounds 4b, 4e, and 4f, demonstrate balanced pharmacokinetic properties with favorable absorption, permeability, and acceptable metabolic profiles, highlighting their potential as promising drug candidates (Tables 3–5).

Table 3: Calculation of ADME properties of compounds 4a-4i using pkCSM

Entry	Log S (log mol/L)	Caco-2 permeability (log Papp ×10⁻⁶ cm/s)	Intestinal absorption (%)	VDss (log L/kg)	Fraction unbound (Fu)	BBB permeability (log BB)	CNS permeability (log PS)	Metabolism (CYP interaction)	Excretion (log ml/min/kg)
4a	-4.51	1.091	100	0.534	0.317	0.448	-1.684	CYP3A4 (S & I), CYP1A2 (I), CYP2C9 (I)	0.893
4b	-2.954	1.158	100	0.322	0.309	1.128	-1.913	CYP3A4 (S & I), CYP1A2 (I)	1.011
4c	-2.939	1.341	100	0.151	0.311	0.749	-2.253	CYP3A4 (S), CYP1A2 (I)	0.995
4d	-2.988	2.031	100	0.033	0.306	-1.18	-2.171	CYP3A4 (S), CYP1A2 (I)	0.971
4e	-2.958	1.156	98.932	0.326	0.306	1.115	-1.872	CYP3A4 (S), CYP1A2 (I)	0.153
4f	-2.961	1.154	98.865	0.332	0.306	1.114	-1.849	CYP3A4 (S & I), CYP1A2 (I)	0.132
4g	-5.334	1.053	99.313	0.346	0.299	0.259	-1.339	CYP3A4 (S), CYP1A2 (I), CYP2C9 (I)	0.825
4h	-2.942	1.320	100	0.295	0.305	-0.829	-2.048	CYP3A4 (S & I), CYP1A2 (I)	1.051
4i	-4.30	1.072	98.229	0.579	0.237	0.244	-1.624	CYP3A4 (S & I), CYP1A2 (I), CYP2C9 (I)	0.831

Table 4: Toxicity prediction of compounds 4a-4i using pkCSM

Entry	AMES Toxicity	hERG I Inhibitor	hERG II Inhibitor	Hepatotoxicity	Skin Permeation	Max. Tolerated Dose (human) log (mg/kg/day)
4a	Yes	No	Yes	Yes	No	0.576
4b	No	No	Yes	Yes	No	0.617
4c	No	No	Yes	Yes	No	0.602
4d	No	No	Yes	Yes	No	0.615
4e	No	No	Yes	Yes	No	0.619
4f	No	No	Yes	Yes	No	0.620
4g	No	No	Yes	Yes	No	0.508
4h	No	No	Yes	Yes	No	0.615
4i	No	No	No	Yes	No	0.111

Table 5: Drug Likeness and Lipophilicity profile of the compounds 4a-4i calculated using SWISS/ADME

Entry	Lipinski Rule	Ghose Rule	Veber Rule	Egan Rule	Muegge Rule	Lipophilicity (Log Po/w)
4a	Yes	Yes	Yes	Yes	Yes	4.03
4b	Yes	Yes	Yes	Yes	Yes	4.35
4c	Yes	Yes	Yes	Yes	Yes	4.02
4d	Yes	Yes	Yes	Yes	Yes	3.44
4e	Yes	Yes	Yes	Yes	No	4.56
4f	Yes	Yes	Yes	Yes	No	4.63
4g	Yes	No	Yes	No	No	5.72
4h	Yes	Yes	Yes	Yes	Yes	3.80
4i	Yes	Yes	Yes	Yes	No	4.32

Table 6: ADMET radar plot analysis of compounds 4a–4i illustrating predicted pharmacokinetic properties and drug-likeness parameters

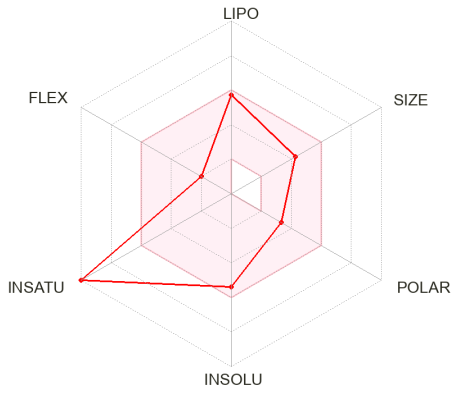

4a

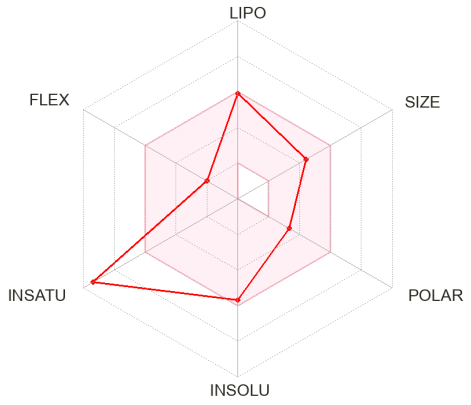

4b

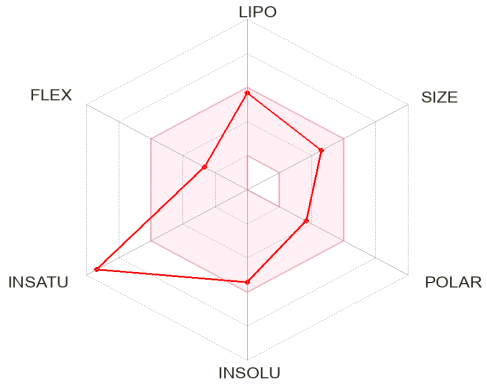

4c

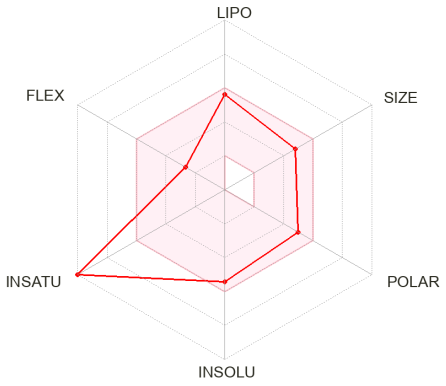

4d

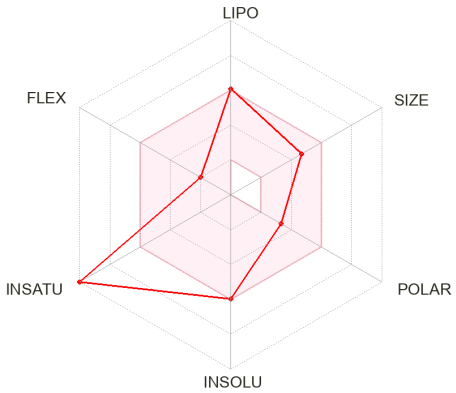

4e

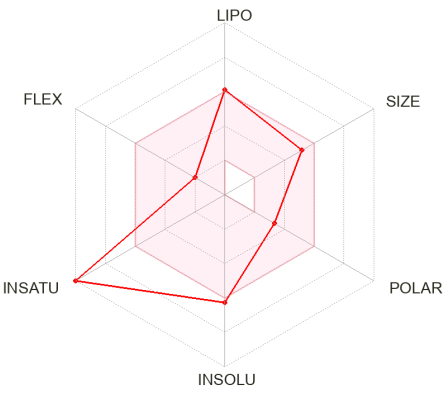

4f

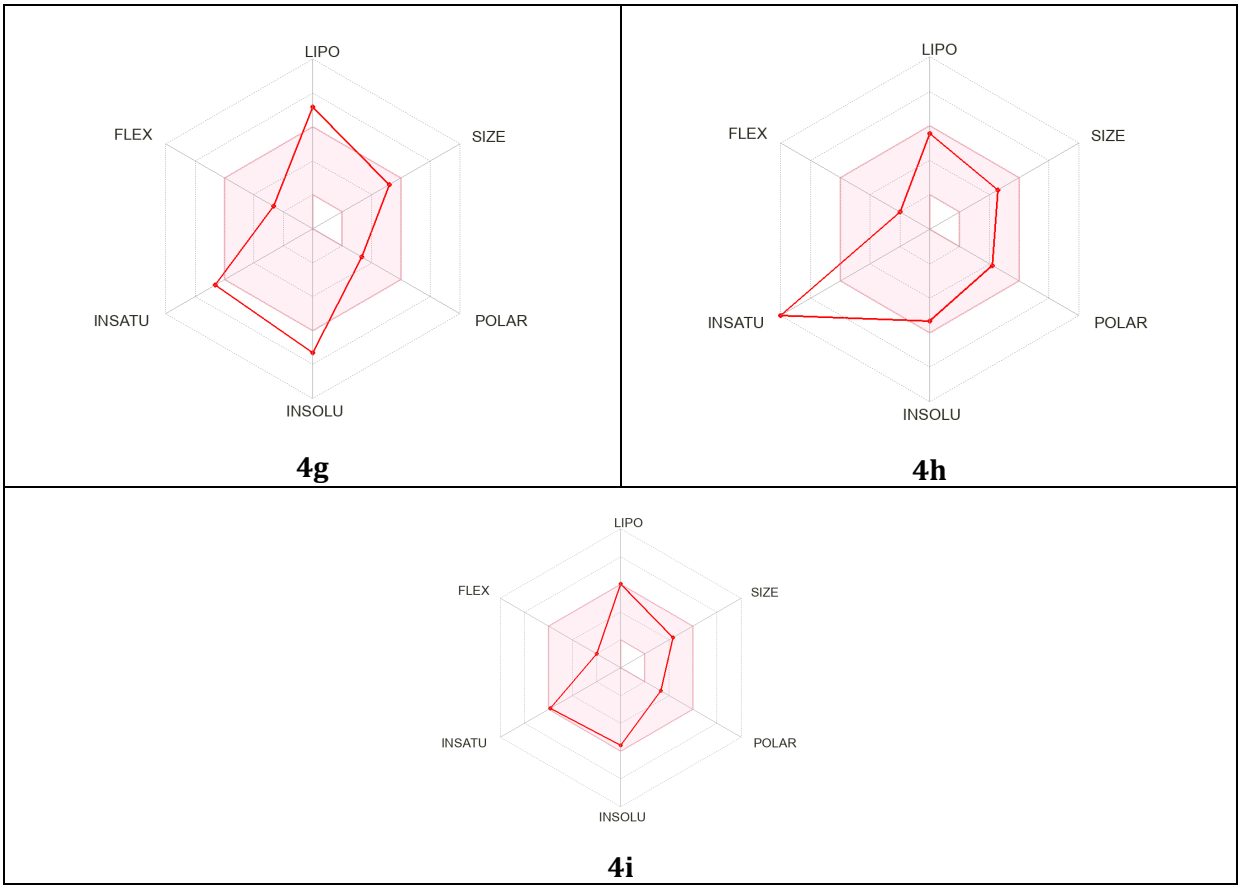

CONCLUSION

Compound 4g exhibited the highest binding affinity -9.79 kcal/mol with the lowest inhibition constant 67.04 nM. Compound 4i also demonstrated strong binding with a docking score of -8.81 kcal/mol. Compound 4h formed two hydrogen bonds with THR165 and VAL167 residues. Compound 4a and 4d formed single hydrogen bonds with THR165 and ARG136, respectively. The observed bond lengths 2.17–2.57 Å indicate stable hydrogen bonding interactions. 4a–4i showed excellent intestinal absorption 98–100%, indicating good oral bioavailability potential. Caco-2 permeability values log Papp 1.05–2.03, suggest moderate to high intestinal permeability, with compound 4d showing the highest permeability 2.031. Water solubility Log S values indicate moderate solubility for most compounds, while 4g -5.334 and 4a -4.51 showed comparatively lower solubility Volume of distribution VDss 0.033–0.579 Log L/kg suggests moderate tissue distribution, with 4i showing the highest distribution profile. Fraction unbound Fu 0.237–0.317 indicates moderate plasma protein binding across all derivatives. BBB permeability log BB shows that compounds 4b, 4e, and 4f possess higher brain penetration potential, whereas 4d and 4h exhibit limited BBB permeability. CNS permeability log PS -1.339 to -2.253 indicates generally low CNS penetration, suggesting reduced central nervous system side effects. Most compounds act as substrates of CYP3A4, indicating hepatic metabolism through this major enzyme.

REFERENCES

1. Surender Reddy S, Shireesha K, Jella KS. [2025]. Synthesis, Biological Evaluation, and Molecular Docking Studies of [1, 8]-Naphthyridine Derivatives as Potential Anticancer and Antimicrobial Agents. Polycycl Aromat Compd.45(10):1988–2001.
2. Mhaibes RM. Synthesis Methods of Calcium Channel Blockers : A Review. [2025]. J Med Med Chem.1:43–7.
3. Lesher GY, Froelich EJ, Gruett MD, Bailey JH, [1962]. Brundage RP. 1,8-Naphthyridine Derivatives. A New Class of Chemotherapeutic Agents. J Med Pharm Chem.5(5):1063–5.
4. Vikedal K, Ræder SB, Riisnæs IMM, Bjørås M, Booth JA, Skarstad K, et al. [2025]. RecN and RecA orchestrate an ordered DNA supercompaction response following ciprofloxacin-induced DNA damage in *Escherichia coli.* Nucleic Acids Res.53(10).
5. Jia ZH, Pilkington LI, Barker D. [2024]. Total Syntheses and Absolute Stereochemical Correction of Negundin B, Vitexin 1, and Vitexin 6. J Org Chem.89(5):3644–51.
6. Wise R, Andrews JM, Danks G. [1984]. In-vitro activity of enoxacin (CI-919), a new quinoline derivative,

compared with that of other antimicrobial agents. J Antimicrob Chemother.13(3):237–44.
7. Jałbrzykowska K, Chrzanowska A, Roszkowski P, Struga M. [2022]. The New Face of a Well-Known Antibiotic: A Review of the Anticancer Activity of Enoxacin and Its Derivatives. Vol. 14, Cancers..
8. Esther Meseko, Etudaiye Anomi, Justice Ovidiohu Adamu.(2026). Antibacterial Potential of Lemon (*Citrus limon*) and Lime C*itrus aurantifolia*) Peel Extracts. Chem Res Technol. In Press.
9. Rubinstein E. [2001]. History of quinolones and their side effects. In: Chemotherapy. p. 3–8.
10. Hellio C, Pons AM, Beaupoil C, Bourgougnon N, Gal Y Le. (2002). Antibacterial, antifungal and cytotoxic activities of extracts from fish epidermis and epidermal mucus. Int J Antimicrob Agents.20(3):214–9.
11. Goldstein EJC, Citron DM, Warren Y, Tyrrell K, Merriam CV. [1999]. In vitro activity of gemifloxacin (SB 265805) against anaerobes. Antimicrob Agents Chemother.43(9):2231–5.
12. Chauffard A, Bridevaux PO, Carballo S, Prendki V, Reny JL, Stirnemann J, et al. [2022]. Accuracy of a score predicting the presence of an atypical pathogen in hospitalized patients with moderately severe community-acquired pneumonia. BMC Infect Dis.22(1).
13. Lang Y, Gong C, Li D. 2025 (). High prevalence and pathogen-specific variations of co-infections in pediatric adenovirus pneumonia: a retrospective epidemiological analysis from Northern China. Ital J Pediatr.51(1).
14. Yague G, Morris JE, Pan XS, Gould KA, Fisher LM. [2002] . Cleavable-complex formation by wild-type and quinolone-resistant *Streptococcus pneumoniae* type II topoisomerases mediated by gemifloxacin and other fluoroquinolones. Antimicrob Agents Chemother.;46(2):413–9.
15. Bowker KE, Noel AR, MacGowan AP. [2006]. Pharmacodynamics of dalbavancin studied in an in vitro pharmacokinetic system. J Antimicrob Chemother.58(4):802–5.
16. López F, Culebras E, Betriú C, Rodríguez-Avial I, Gómez M, Picazo JJ. [2010]. Antimicrobial susceptibility and macrolide resistance genes in *Enterococcus faecium* with reduced susceptibility to quinupristin-dalfopristin: level of quinupristin-dalfopristin resistance is not dependent on erm(B) attenuator region sequence. Diagn Microbiol Infect Dis.66(1):73–7.
17. Park HS, Oh SH, Kim HS, Choi DR, Kwak JH. [2016]. Antimicrobial activity of zabofloxacin against clinically isolated Streptococcus pneumoniae. Molecules.21(11).
18. 18. Khan SL, Bakshi V. [2026]. Physicochemical characterization , GC – MS profiling , and computational evaluation of *Ailanthus excelsa* hydroalcoholic extract against mutant EGFR. Chem Rev Lett.9:358–76.
19. Chaudhari RN, L.Khan S, Chaudhary RS, Jain SP, Sidduqui FA. [2020]. B-Sitosterol: Isolation From Muntingia Calabura Linn Bark Extract, Structural Elucidation And Molecular Docking Studies As Potential Inhibitor Of Sars-CoV-2 Mpro (COVID-19). Asian J Pharm Clin Res.204–9.
20. Khan SL, Siddiqui FA, Jain SP, Sonwane GM. [2021] . Discovery of Potential Inhibitors of SARS-CoV-2 (COVID-19) Main Protease (Mpro) from Nigella Sativa (Black Seed) by Molecular Docking Study. Coronaviruses.2(3):384–402.
21. Siddiqui FS. [2026]. Computational Assessment of Secondary Metabolites as Potential Inhibitors of Methylenetetrahydrofolate Dehydrogenase-2 (MTHFD2). J Phytopharm Adv Chem.2:3–17.
22. Jadhav PB, Jadhav SB, Zehravi M, Mubarak MS, Islam F, Jeandet P, et al. [2023]. Virtual Screening, Synthesis, and Biological Evaluation of Some Carbohydrazide Derivatives as Potential DPP-IV Inhibitors. Molecules.28(1). 24